ISSN 1068-3755, Surface Engineering and Applied Electrochemistry, 2018, Vol. 54, No. 3, pp. 267–272. © Allerton Press, Inc., 2018.
Original Russian Text © A.K. Shuaibov, M.P. Chuchman, L.V. Mesarosh, 2018, published in Elektronnaya Obrabotka Materialov, 2017, No. 3, pp. 41–46.

Electrical Characteristics of a Glow Discharge in Air over the Surface of Aluminum Sulfate Aqueous Solution

A. K. Shuaibov[a], *, M. P. Chuchman[a], and L. V. Mesarosh[a]

[a] *Uzhgorod National University, Uzhgorod, 88000 Ukraine*

**e-mail: alexsander.shuaibov@uzhnu.edu.ua*

Received May 18, 2016; in final form, February 3, 2017

Abstract—The paper presents the current–voltage characteristics, the magnitudes of cathode potential drop, the dependences of the total and specific glow discharge power which is injected into the plasma from the discharge current, as well as the density of electrons in the glow discharge in air at atmospheric pressure with the cathode based on 1–10% solutions of aluminum sulfate in distilled water. The distance between the electrolytic liquid cathode and the metal anode is varied from 1 to 10 mm at an average discharge current of 8–36 mA. The discharge is promising for the synthesis of nanostructures of aluminum and aluminum oxide which are formed when processing the solutions with a glow discharge.

Keywords: glow discharge with liquid cathode, aluminum sulfate aqueous solution, electrical characteristics

DOI: 10.3103/S1068375518030122

INTRODUCTION

A glow discharge in free air between a metal anode and water or liquid electrolytic cathode is distinguished by simple implementation and control of plasma parameters, inexpensive materials, many various applications in plasma chemistry, as well as the conversion of chemical compounds within the discharge bulk and on the liquid surface. In ecology, it is used to purify air and water, to utilize harmful wastes, in medicine and agriculture, to modify surfaces of various materials, as well as to synthesize nanoparticles of metals and their oxides [1–8]. This glow discharge plasma is strongly nonequilibrium, it serves as a source of radicals of hydroxyl, hydrogen peroxide, nitrogen oxides, as well as atoms of hydrogen and oxygen that can be used to synthesize nanostructures of metal oxides. As the greater part of this plasma radiation is concentrated in the ultraviolet region, it has been proposed to design a simple windowless long-lived lamp using the noncarcinogenic UV radiation from the hydroxyl radical bands and the second positive system of a nitrogen molecule [9]. In the case of plasma–chemical open–type reactors, it is important that there is a steady-state discharge in free air for diffuse plasma formation so no expensive vacuum equipment is required.

Works [10, 11] reported a successive synthesis of small copper and nickel nanoparticles (up to 10–30 nm) in the spark discharge in free air over the surface of copper and nickel sulfate aqueous solutions. In these experiments, the dimensions and the yield of nanoparticles greatly depend on the discharge device circuit, the electrolytic cathode properties, as well as the characteristics and parameters of plasma formed over the electrolyte.

At present, there is no glow discharge in free air over the surface of the aluminum sulfate distilled aqueous solution whose characteristics and parameters are promising for synthesis of Al_2O_3 aluminum oxide nanostructures in a macroscopic amount. In comparison with the synthesis of the metal oxide nanostructures in a nanosecond discharge in distilled water the glow discharge over the surface of a metal-containing salt solution has a number of advantages: lower working voltage, a simple source of discharge ignition, and no automated system of maintaining the interelectrode gap [12]. Aluminum oxide-based nanostructures are widely used in modern micronanoelectronics [13].

This paper presents the electrical characteristics and parameters of a glow discharge in free air with the cathodes based on aluminum sulfate distilled aqueous solutions. This discharge is promising for use in the open-type plasma-chemical gas discharge reactors with possible synthesis of nanostructures based on aluminum oxide in a macroscopic amount.

EXPERIMENTAL

A glow discharge in free air was ignited over the surface of the solution of aluminum sulfate ($Al_2(SO_4)_3$) in distilled water in a Plexiglas cuvette. The test bench diagram is presented in [9, 14]. The metal anode placed over the surface of electrolyte in air was made

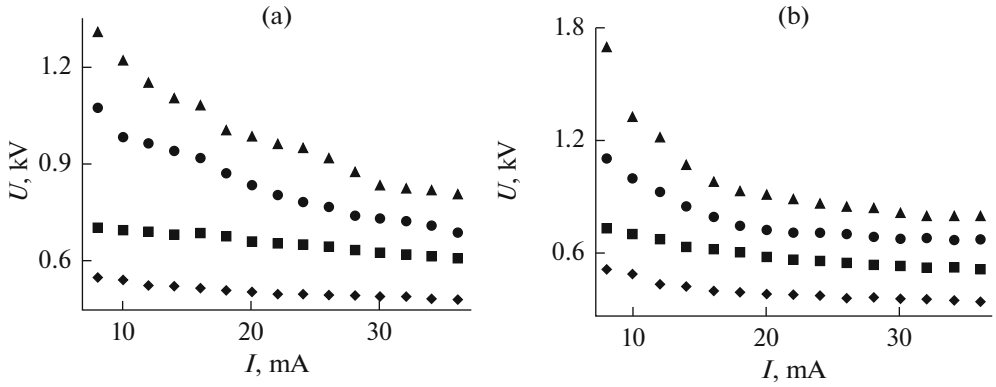

Fig. 1. Current–voltage characteristics of a glow discharge with an electrolytic cathode based on aluminum sulfate aqueous solution in distilled water (1 (a), 10% (b)) with different spacings between the solution surface (◆ 1, ■ 3, ● 5, ▲ 7 mm) and metal anode.

in the form of a copper needle 2 mm in diameter. The copper anode was attached in a special mobile device to vary the spacing between the needle tip and the electrolyte surface from 1 to 12 mm. The second copper electrode in the form of a plate was situated in the electrolyte. The distance between the upper plate metal surface and the electrolyte surface could be varied from 1 to 10 mm. The container volume was about 10^3 cm^3. The main experiments were carried out at an anode tip-electrolyte surface spacing of 7 mm and a solution thickness of 5 mm over the metal cathode surface. A high-voltage rectifier with the peak output characteristics (voltage U = 1–25 kV; current I = 1–100 mA) was used to ignite a glow discharge. A ballast resistance of R = 434 kΩ was used to stabilize the glow discharge.

The geometrical dimensions of the glow discharge were determined imaging (digital camera Olympus FE-25/X-20) the corresponding plasma formation at different currents. The electric glow discharge power was determined according to the current–voltage characteristics measured using an C-196 kilovoltmeter and a M 906 milliammeter.

CHARACTERISTICS AND PARAMETERS OF A GLOW DISCHARGE

The spatial characteristics of the glow discharge in free air over the surface of the $Al_2(SO_4)_3$ solution in distilled water (1–10% of salt in water) for different metal anode–electrolyte surface spacings and different depths at which the metal cathode was arranged in the solution at currents I = 8–34 mA were close to the corresponding data for the glow discharge with the cathode based on the solution of copper sulfate in water [15]. The highest plasma radiation intensity was achieved at the discharge currents I = 20–34 mA, an interelectrode spacing of d = 7 mm, and at the depth of the metal cathode arrangement of $h \approx 5$ mm. The diameter of the cathode spot for the cathode based on 1–10% aluminum sulfate solutions stayed within 3–4.5 mm.

The current–voltage characteristics (CVCs) of the glow discharge in air with a liquid electrolytic cathode are presented in Fig. 1. The CVCs of the glow discharge with an electrolytic cathode were similar to the CVCs of the glow discharge over the surface of distilled water produced using the same installation [16] and the CVCs of the longitudinal discharge in low-pressure gases with metal electrodes which had the expressed subnormal and normal stages [17]. With the increase in the solution concentration and the interelectrode gap (d > 3 mm), the voltage drop in the discharge gap became sharper with the increase in the current, which indicates the more important role of the subnormal discharge stage. The independence of the voltage drop in the gap on the current value (normal combustion mode) for the glow discharge with an electrolytic cathode mostly manifested itself within the range from 24 to 36 mA for the 10% solution of $Al_2(SO_4)_3$ in distilled water at d = 7 mm.

The change in the ignition potential versus the interelectrode gap was studied in work [18]. The correlation of the discharge ignition potential [18] and the voltage at a current of 8 mA at an interelectrode gap from 1 to 7 mm is shown in Fig. 2 for water, 1 and 10% $Al_2(SO_4)_3$ solutions. The breakdown voltage greatly decreases when the interelectrode gap is reduced. The voltage at small discharge currents is similar. It grows considerably with the increase in the interelectrode gap. At an interelectrode gap of 1 mm and a current of 8 mA the voltage in the discharge gap in all the cases was similar (~ 0.6 kV). The breakdown voltage at an interelectrode gap of 1 mm is 1.2 kV, and at an interelectrode gap of 3 mm it is 5.2 kV in the case of water [18].

With an increase in the aluminum sulfate content in distilled water from zero to 10%, the variation in the voltage in the discharge gap is not monotonic. Thus, for example, at d = 7 mm, I = 8 mA for the cathode

based on 1% $Al_2(SO_4)_3$ solution it is about 1.3 kV, and for the cathode based on 10% $Al_2(SO_4)_3$ solution it is ≈1.75 kV. Under the same conditions, the voltage for the glow discharge over the distilled water surface was ≈1.5 kV [16]. This indicates the interrelation between the electrolyte properties and the discharge characteristics.

The procedure presented in work [16] was used to determine the magnitude of the drop of the potential (U_C) at the cathode in the glow discharge with electrolytic cathodes at different concentrations of the $Al_2(SO_4)_3$ salt in distilled water based on the measured CVCs (Fig. 3). For the 10% $Al_2(SO_4)_3$ solution, the potential drop at the cathode is about 40 V less than for the cathode based on distilled water, though the form of the dependence of U_C on the discharge current was similar. The greatest differences of the U_C values for the cathodes with the 1 and 10% salt concentrations in water were observed with the discharge currents in the range from 10 to 20 mA. The U_C value for the cathode with the 10% salt concentration at low currents (<30 mA) was more than for the cathode based on the 1% solution. For the cathode based on distilled water, the highest value U_C = 495 V was achieved at a discharge current of 12 mA, and with the current increase it was reduced to 440 V [15].

The electric power of the glow discharge was the highest for the cathode based on distilled water (Fig. 4). With the increase in the solution concentration, less power is put into the glow discharge, and a decrease in its volume is observed. With the glow discharge current increasing from 12 to 32 mA, the electric power of the discharge increased from 16 to 31 W, and in the range from 14 to 26 W for the cathode based on distilled water and 10% $Al_2(SO_4)_3$ solution, respectively. The discharge volume was 64–80 and 49–63 mm^3, respectively.

At present, the physical processes in the plasma of the glow discharge with liquid nonmetal electrodes are little studied, which retards the development and improvement of the operation of various plasma chemical reactors. For advances in this direction, it is necessary to know the main parameters of this plasma (density n_e and electron temperature T_e) in free air, as well as their dependences on the reactor characteristics (interelectrode gap, solution concentration, current value, etc.).

In [19, 20], by probing the plasma with microwave radiation and the probe technique, estimates of the electron density and temperature for a glow discharge in air between two electrodes based on technical water were made. In the center of the interelectrode gap (d = 6 mm) the electron density value was about 10^{12} cm^{-3} (at currents 60–100 mA), and the electron temperature was 0.4 eV.

The parameters of the glow discharge in free air over the surface of aluminum-containing salts in distilled water were not studied earlier. The estimation procedure for electron density in the glow discharge over the electrolyte surface is described in [12], and the results were reported at the international conference [21].

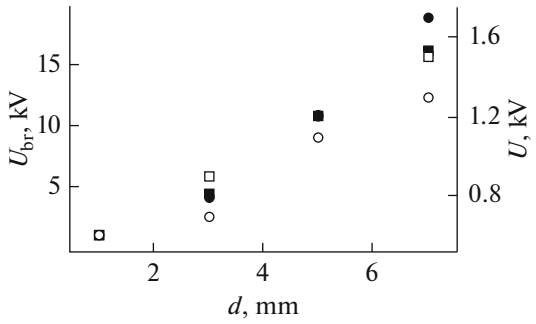

Fig. 2. Correlation of breakdown voltage (U_{br}) for water ■ and voltage with a discharge current of 8 mA for water □, 1 ○ and 10% ● aluminum sulfate solutions.

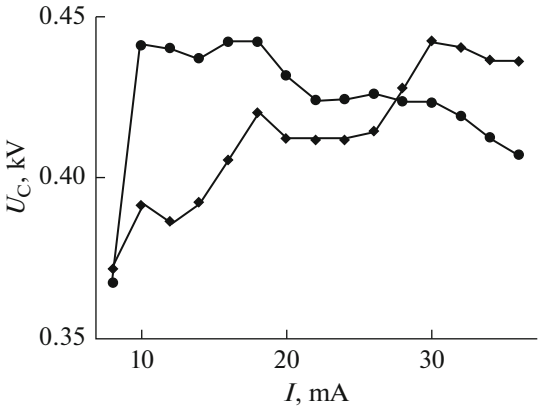

Fig. 3. Cathode potential drop in the glow discharge with liquid cathode versus discharge current magnitude with different content of aluminum sulfate in water: ◆ 1, ● 10%.

The electron density in parts of the different glow discharge were estimated according to the value of the measured current (I) which is proportional to the magnitude of the electric charge passing through the cross section of a conductor S in area:

$$I = en_e v_{dr} S, \quad (1)$$

where e is the electron charge, n_e is the electron density, and v_{dr} is the electron drift velocity [17]. In formula (1), we take account of the fact the current in the discharge is formed mostly by the electrons as their mobility is three orders of magnitude more than the mobility of ions. The electron density was defined by the following formula:

$$n_e = (I/S)(1/ev_{dr}), \quad (2)$$

The electron drift velocity in the discharge can be presented in the form of the product of the electric field intensity (E) and the electron mobility (μ) v_{dr} =

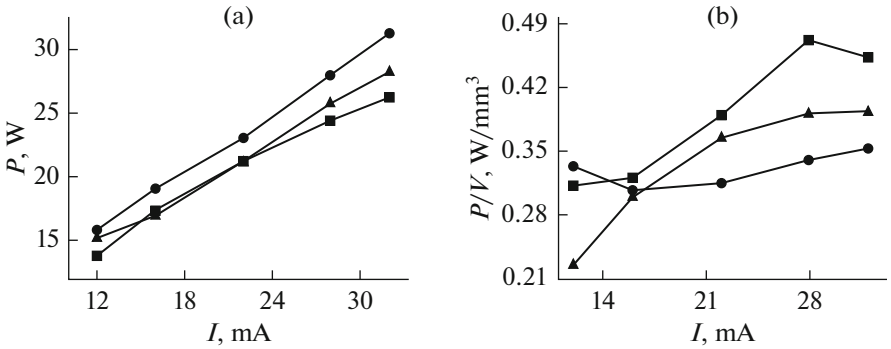

Fig. 4. Dependence of total electrical (a) and specific electrical (b) powers put in glow discharge plasma on current magnitude for electrolytic cathode: ▲ 1% $Al_2(SO_4)_3$ solution; ■ 10% $Al_2(SO_4)_3$ solution; ● distilled water.

μE, where $\mu = (2el/mE)^{0.5}$ (here l is the electron free path and m is the electron mass). The electric field intensity can be estimated from the formula $E = E_i/el$ where E_i is the nitrogen molecule ionization energy. The electron free path length can be estimated through the diameter D and the nitrogen molecule density n_{N2} ($n_{N2} = p/kT$): $l = 1/(2^{0.5}\pi D^2 n_{N2})$.

In any gas at low currents, the anode potential drop (U_A) is significantly smaller than the cathode potential drop: $U_A \ll U_C$ [12, 17]. The measured experimental CVCs of the glow discharge were used to determine the cathode potential drop and the voltage drop in the discharge gap: $U = U_C + U_A + U_{PC}$, where U_{PC} is the voltage drop in the positive column of glow discharge.

The cathode potential drop was determined at the fixed discharge current in the anode–electrolyte gap as a function of the cathode–anode spacing. The extrapolation of this function to the zero spacing gave the value of the cathode potential drop U_C.

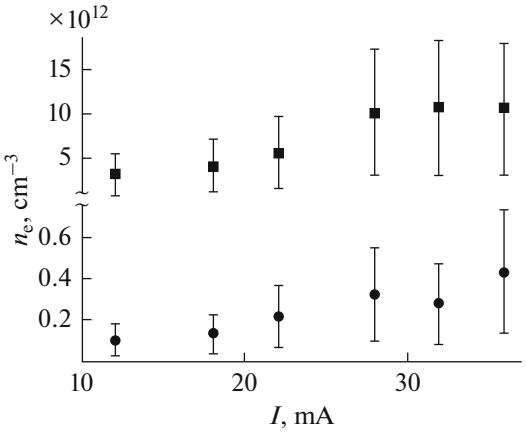

Fig. 5. Electron density in positive column (●) and cathode part (■) of glow discharge over the surface of 10% $Al_2(SO_4)_3$ solution versus current magnitude.

In the region of positive column, the electron density value is the lowest. To estimate the electric field intensity in the positive column of glow discharge, the following formulas were used:

$$U_A \ll U_C, \quad U_{PC} = U - U_C. \tag{3}$$

Knowledge that, according to collision theory, the size of the cathode and anode layer is about 10^{-6} m [17], the electric field intensity in the positive column can be estimated from the relation $(U - U_C)/d$, where d is the interelectrode spacing. The error of the electron concentration computation within the proposed model is 30%.

The value of the glow discharge cross-sectional area in the region of the cathode spot and the positive column was estimated using the plasma formation pictures.

The preliminary experiment with the cathode based on distilled water allowed the estimation of electron density in the cathode part and the positive column of the glow discharge for currents within the range from 10 to 32 mA [22]. Thus, the value n_e in the discharge cathode part increased (from 2 to 10) × 10^{12} cm^{-3} with the increase in current. The electron density for the positive column in the current range from 10 to 20 mA also increased (from 1 to 2) × 10^{11} cm^{-3}. At the currents over 20 mA, the value n_e became stable at the level of 2 × 10^{11} cm^{-3}.

The increase in the electron density in the cathode part of the glow discharge against a slight change in the cathode spot diameter indicates the formation of molecules with small ionization potentials in the cathode layer. In our case these can be NO radicals.

The dependences of the electron density in different parts of the discharge on the current for the 10% aluminum sulfate solution are presented in Fig. 5. With the increase in the discharge current from 12 to 36 mA, the value n_e grew in the range (1–4) × 10^{11} cm^{-3} (the positive discharge column) and (3–10) × 10^{12} cm^{-3} (the cathode layer) for the currents from 12 to 27 mA. For the currents $I > 27$ mA, the value n_e in the cathode layer became saturated at a level of 10^{13} cm^{-3}. The increase

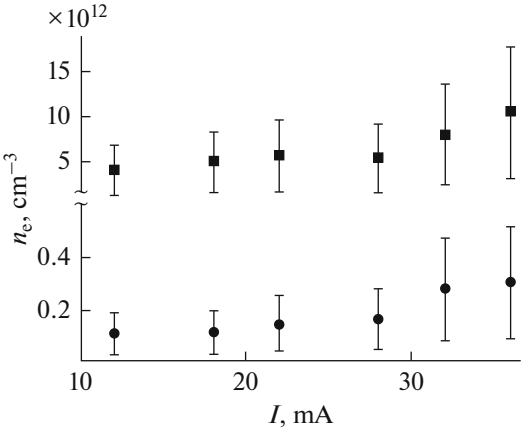

Fig. 6. Electron density in plasma of positive column (●) and cathode region (■) of glow discharge over the surface of 1% $Al_2(SO_4)_3$ solution versus current magnitude.

in the electron density in glow discharge over the surface of the salt solution in comparison with the discharge with a water cathode is connected with the increase in the conductivity of the solution and the appearance of molecules with a low ionization potential due to the electrolytic dissociation in the solution (SO gas can evolve) and plasma-chemical reactions (synthesis of NO).

The results can be compared with the data in [23], where in the central part of the atmospheric-pressure discharge plasma in the glow discharge with an electrolytic cathode $n_e = 7 \times 10^{12}$ cm^{-3}.

For the discharge with the cathode based on the 1%-salt solution, the electron density in the cathode layer and the positive column are presented versus current in Fig. 6. The values of n_e for this discharge (1% solution) for the cathode layer and the positive column of the glow discharge with the increase in current increased within the range 4×10^{12}–1×10^{13} and 1.1×10^{11}–3×10^{11} cm^{-3}, respectively.

As seen from Figs. 5 and 6, for the glow discharge with the cathodes based on the solution, a great increase in the electron density is observed at currents of $I > 25$–28 mA. After 25 mA, the plasma chemical reactions and the electrolytic dissociation begin to be manifest, which results in the change in the discharge color.

The electrolytic dissociation can be presented by the following equations: $H_2O = H^+ + OH^-$, $Al_2(SO_4)_3 = 2Al^{3+} + 3SO_4^{2-}$. Negative ions formed as a result of the electrolytic dissociation (OH^-, SO_4^{2-}) and secondary processes in the electrolyte (AlO_2^-) will enrich its surface layer. The reactions of the plasma and electrolyte components with the mentioned radicals, their oxidation and decomposition will determine the change in the composition of both electrolyte and plasma. As a consequence, within the discharge gap, SO molecules will appear which contribute to the specific nature of the combustion discharge, its characteristics and parameters.

CONCLUSIONS

Thus, the study of a glow discharge with an electrolytic liquid cathode showed that in free air at currents 8–36 mA the discharge exists in the form of a diffusion channel; the breakdown voltage with a reduction in the interelectrode gap greatly decreases, and the voltage at low discharge currents nonmonotonically depends on the concentration of aluminum sulfate in the solution and varies from 1.3 (1% solution) to 1.75 kV (10% solution) though the combustion potential of the discharge over the distilled water surface was 1.5 kV under the same conditions; the potential cathode drop at currents from 8 to 36 mA changed from 370 to 450 V, and it was high for the more concentrated solution with currents up to 30 mA; with the increase in the solution concentration, lower power was injected into the discharge at the highest current (from 31 to 26 W) and the decrease in its volume was observed (from 80 to 63 mm^3), For the solutions, the value n_e increased with the increase in current and attained 4×10^{11} cm^{-3} (the positive discharge column) and 10^{13} cm^{-3} (the cathode layer). To increase the yield of nanostructures, increases in the current and discharge area are desirable, with studies of the influence of plasma UV radiation intensity on their formation.

REFERENCES

1. Gaisin, F.M. and Son, E.E., *Entsiklopediya nizkotemperaturnoi plazmy* (Encyclopedia of Low-Temperature Plasma), Moscow: Nauka, 2000, vol. 2, pp. 241–246.
2. Gaisin, A.F., Abdullin, I.Sh., and Gaisin, F.M., *Struinyi mnogokanal'nyi razryad s elektroliticheskimi elektrodami v protsessakh obrabotki tverdykh tel* (Jet Multi-Channel Discharge with Electrolytic Electrodes in the Processing of Solids), Kazan: Kazansk. Gos. Tekh. Univ., 2006, 446 p.
3. Valiev, R.I., Shakirov, B.Yu., and Shakirov, Yu.I., *Vektor Nauki Tol'yatt. Gos. Univ.*, 2012, vol. 1, no. 19, pp. 54–57.
4. Zhilinskii, V.V., Drozdovich, V.B., Ivanova, N.P., and Zhdanok, S.A., *Vestsi Akad. Navuk Belarusi, Ser. Khim. Navuk*, 2010, no. 1, pp. 12–15.
5. Richmonds, C. and Sankaran, R.M., *Appl. Phys. Lett.*, 2008, vol. 93, p. 132501.
6. Kuz'micheva, L.A., Titova, Yu.V., and Maksimov, A.I., *Elektron. Obrab. Mater.*, 2006, no. 3, pp. 148–152.
7. Orlov, A.M., Yavtushenko, I.O., and Bodnarskii, D.S., *Tech. Phys.*, 2012, vol. 57, no. 3, pp. 386–391.
8. Kulentsan, A., Rybkin, V., Titov, V., and Smirnov, S., *Proc. of the 28 Int. Conf. on Phenomena in Ionized Gases (28th ICPIG)*, Prague, 2007, pp. 2282–2284.

9. Shuaibov, A.K., Chuchman, M.P., Mesarosh, L.V., and Grabovaya, I.A., *Instrum. Exp. Tech.*, 2013, vol. 56, no. 6, pp. 726–730.
10. Orlov, A.M., Yavtushenko, I.O., Bodnarskii, D.S., and Ufarkina, N.V., *Tech. Phys.*, 2013, vol. 58, no. 9, pp. 1267–1273.
11. Orlov, A.M., Yavtushenko, I.O., Bodnarskii, D.S., *Tech. Phys.*, 2015, vol. 60, no. 5, pp. 710–716.
12. Mesarosh, L.V. and Shuaibov, O.K., *Aktual'ni problemi kvantovoi fiziki. Praktiku, z laboratornikh robit* (Relevant Problems in Quantum Physics. Practical Manual), Uzhgorod: Goverla, 2015, 84 p.
13. Golovan, L.A., Timoshenko, V.Yu., and Kashkarov, P.K., *Phys.-Usp.*, 2007, vol. 50, no. 6, pp. 595–612.
14. Mesarosh, L.V., Shuaibov, O.K., Chuchman, M.P., *Nauk. Visn. Uzhgorod. Univ., Ser. Fiz.*, 2012, no. 32, pp. 82–88.
15. Shuaibov, A.K., Chuchman, M.P., and Kozak, Ya.Yu., *Usp. Prikl. Fiz.*, 2014, vol. 2, no. 1, pp. 41–44.
16. Shuaibov, A.K., Chuchman, M.P., and Mesarosh, L.V., *Tech. Phys.*, 2014, vol. 59, no. 6, pp. 847–851.
17. Raizer, Yu.P., *Fizika gazovogo razryada* (Physics of Gas Discharge), Moscow: Nauka, 1987, 592 p.
18. Bruggeman, P., Graham, L., Degroote, J., Vierendeels, J., et al., *J. Phys. D: Appl. Phys.*, 2007, vol. 40, pp. 4779–4786.
19. Barinov, Yu.A., Kaplan, V.B., Rozhdestvenskiĭ, V.V., and Shkol'nik, S.M., *Tech. Phys. Lett.*, 1998, vol. 24, no. 12, pp. 929–931.
20. Barinov, Yu.A. and Shkol'nik, S.M., *Tech. Phys.*, 2002, vol. 47, no. 3, pp. 313–319.
21. Mesarosh, L.V., Shuaibov, O.K., and Chuchman, M.P., *Materiali mizhnarodnoi naukovoi konferentsii molodikh vchenikh i aspirantiv "IEF-2015"* (Proc. Int. Sci. Conf. of Young Scientists and Post-Graduate Students "IEF-2015"), Uzhgorod, 2015, pp. 81–82.
22. Shuaibov, O.K., Mesarosh, L.V., and Chuchman, M.P., *Tekh. Elektrodin.*, 2016, no. 2, pp. 25–28.
23. Mezei, P. and Cserfalvi, T., *Appl. Spectrosc. Rev.*, 2007, vol. 42, no. 6, pp. 573–604.

Translated by M. Myshkina